JOURNAL OF THEORETICAL
AND APPLIED MECHANICS
41, 3, pp. 443-457, Warsaw 2003

ELASTO-PLASTIC LIMIT LOADS OF CYLINDER-CONE CONFIGURATIONS

Dieter Dinkler
Oliver Knoke

Institut für Statik, Technische Universität Braunschweig
d.dinkler@tu-bs.de, o.knoke@tu-bs.de

The paper presents a procedure for computation of the limit loads of imperfection-sensitive shells including plastic deformations. On the basis of strain energy of shells, the worst case scenario for critical perturbations at fixed load levels is investigated. Limit loads of cylindrical and conical shells under combined actions are compared to European design rules. The concept is applied to more general buckling cases of combined shell structures.

Key words: stability, buckling, imperfection sensitivity, perturbation, plasticity

1. Introduction

Imperfection-sensitivity is a widely discussed phenomenon of thin-walled structures under shear or compression. Many investigations have been presented in this field pursuing the aim to improve the predictability of failure loads that are of interest for design. Thus, publications are dealing very often with safety design concepts for light-weight structures and their experimental and numerical validation. In practice, the shell structures may be complex in geometry, boundaries and loading or may consist of different single shells. For applicability of the design rules, the combined shell structures have to be reduced to uncoupled single substructures. Here the constructional requirements for rigid boundaries arise, what requires expensive ring stiffeners in order to decouple the buckling behaviour of the shell.

In contrast to classical concepts of the bifurcation theory, a perturbation theory has been first developed by Kröplin *et al.* (1985) and applied to numerical investigations of imperfection-sensitive cylindrical shells. Improvements lead to a design model for structures under static loads presented by Duddeck *et al.* (1990). A more general model is presented in Dinkler (1992) for structures under time-dependent perturbations. The perturbation theory is used for cylindrical and conical shells, but could be also applied to more complex buckling cases, if their behaviour is comparable to the known buckling cases. The perturbation theory leads to a proper prediction of buckling loads of realistic structures and fulfil the safety requirements of the design rules.

2. Model equations

A mixed formulation of the governing equations including elasto-plastic material properties is applied to describe the deformation behaviour of thin shells. Under the assumption of moderate rotations and elastic material behaviour, the mixed formulation of the Kirchhoff-Love shell theory including geometrical nonlinearities is given by

$$\begin{aligned}\Pi = \int\limits_A \Big\{\alpha_{\alpha\beta}\widetilde{n}^{\alpha\beta} + \varphi_\beta m^{\alpha\beta}\Big|_\alpha - \frac{1}{2}\widetilde{n}^{\alpha\beta}D_{\alpha\beta\rho\lambda}\widetilde{n}^{\rho\lambda} - \frac{1}{2}m^{\alpha\beta}B_{\alpha\beta\rho\lambda}m^{\rho\lambda}\Big\}\,dA - \\ - \int\limits_A \Big\{u_\alpha\overline{p}^\alpha + u^3\overline{p}_3\Big\}\,dA + \int\limits_{s_u} m^\beta\overline{\varphi}_\beta\,ds - \int\limits_{s_\sigma}\Big\{u_\alpha\overline{n}^\alpha + u^3\overline{n}_3\Big\}\,ds\end{aligned} \tag{2.1}$$

The effects of stresses normal to the shell surface and rotations around the axes normal to shell's surface are neglected. $D_{\alpha\beta\rho\lambda}$ and $B_{\alpha\beta\rho\lambda}$ are the membrane and bending flexibility, respectively. Symmetrical normal forces $\widetilde{n}^{\alpha\beta}$ are defined by

$$\widetilde{n}^{\alpha\beta} = n^{\alpha\beta} + b^\alpha_\rho m^{\rho\beta} \tag{2.2}$$

and strains and slopes of the middle surface by

$$\begin{aligned}\alpha_{\alpha\beta} &= \frac{1}{2}\Big(u_\alpha\Big|_\beta + u_\beta\Big|_\alpha - 2b_{\alpha\beta}u^3 + \varphi_\alpha\varphi_\beta\Big) \\ \varphi_\alpha &= u^3{}_{,\alpha} + b^\rho_\alpha u_\rho\end{aligned} \tag{2.3}$$

Primary variables are the stress resultants $\widetilde{n}^{\alpha\beta}$, $m^{\alpha\beta}$ and displacements u_α, u^3. States of equilibrium satisfy the condition $\Pi \to$ stationary and $\delta\Pi = 0$.

Yield conditions for stress resultants have been first discussed by Ilyushin (1947, 1956). A model to consider the plastification through the cross-section is given by Eggers and Kröplin (1978). It is developed on the basis of the von Mises yield condition, which couples the stress tensor with the one-dimensional yield stress. For the given shell model, yielding produced by normal forces and moments is considered. The elastic limit state Y_0 and plastic limit state Y_1 of the cross-section may be written in terms of the cross-section as

$$\begin{aligned} Y_0 &= \frac{1}{2}\Big(A_{11} + 3|A_{12}| + \frac{9}{4}A_{22} - S_0\Big) = 0 \\ Y_1 &= \frac{1}{2}\Big(A_{11} + \frac{1}{2}A_{22} + \sqrt{(A_{12})^2 + \Big(\frac{1}{2}A_{22}\Big)^2} - S_1\Big) = 0 \end{aligned} \tag{2.4}$$

with

$$\begin{aligned} A_{11} &= n^{\alpha\beta}\, J_{\alpha\beta\rho\lambda}\, n^{\rho\lambda} \\ A_{12} &= \frac{4}{t} n^{\alpha\beta}\, J_{\alpha\beta\rho\lambda}\, m^{\rho\lambda} \\ A_{22} &= \frac{16}{t^2} m^{\alpha\beta}\, J_{\alpha\beta\rho\lambda}\, m^{\rho\lambda} \end{aligned} \tag{2.5}$$

and with the one-dimensional reference forces $S_0 = S_1 = f_y t$, where f_y is the yield stress, t is the shell thickness. The non-zero elements of the material tensor $J_{\alpha\beta\rho\lambda}$ are for isotropic von Mises yielding

$$J_{\alpha\alpha\alpha\alpha} = 1.0 \qquad J_{\alpha\alpha\beta\beta} = -\frac{1}{2} \qquad J_{\alpha\beta\alpha\beta} = \frac{3}{4} \qquad \alpha \neq \beta \tag{2.6}$$

By increasing of the normal forces and moments, the yield surface changes gradually from the elastic limit $(2.4)_1$ to the plastic limit $(2.4)_2$. Intermediate states are approximated by the yield condition

$$Y = \frac{bY_0 + \varepsilon^a Y_1}{b + \varepsilon^a} = 0 \tag{2.7}$$

with the normalized equivalent strain

$$\varepsilon = \frac{\varepsilon_{eq}^{pl}}{\varepsilon_{eq}^{el}} \tag{2.8}$$

For ideal elasto-plastic material behaviour, the parameters a and b are determined by comparison to a layer model; we obtain

$$a = \frac{9}{10} \qquad b = \frac{1}{15} \tag{2.9}$$

To consider the elasto-plastic material behaviour Eq. (2.1) is constrained by the yield condition Y. In order to take into account the path-dependency of plastic strains, the rate formulation of the potential is extended to

$$d\Pi_{tot} = d\Pi - \int_A (dY \cdot d\lambda)\, dA \to \text{stationary} \tag{2.10}$$

with the total differential dY of the yield condition and the Lagrangian multiplier $d\lambda$. $d\Pi_{tot}$ is interpreted as the elasto-plastic potential. Integration over the artificial time interval Δt yields the incremental formulation

$$\Delta\Pi_{tot} = \Delta\Pi - \int_A (\Delta Y \cdot \Delta\lambda)\, dA \to \text{stationary} \tag{2.11}$$

which is the basis for numerical investigations. Variation of the incremental potential leads to the extended governing equations of Prandtl-Reuss type and to the consistency condition.

3. Perturbation theory and limit load criteria

Perturbations or imperfections of ideal configurations may be of different kind with respect to loads, geometry and material. Fig. 1a shows the load-deformation behaviour of axially loaded cylindrical shells for different geometrical imperfections g_p. Increasing the amplitude g_p of geometrical imperfections leads decreasing of the load maximum P. Considering a plane at a certain load level P_0 perpendicular to the load axis, the behaviour of a snap-through becomes obvious, see Fig. 1c. F denotes the fundamental state of equilibrium, M the maximum of restoring forces, N the unstable state of equilibrium in the neighbourhood of F. Stable states S belong to the deep post-buckling region.

In case of perturbation loads orthogonal to the design load a completely similar behaviour can be observed. In dependence on the axial load level, the behaviour with respect to perturbation loads may be interpreted as a snap-through as before, see Fig. 1b. This means that perturbation loads and imperfections may be interpreted by a similar model and may lead to the same process and deformation behaviour and could therefore be evaluated by the same mechanical measure.

Consider a perfect shell under a certain fundamental load level P_0 at which certain states of equilibrium in the post-buckling region exist. The perturbation of the fundamental state of equilibrium F may lead to a transition from

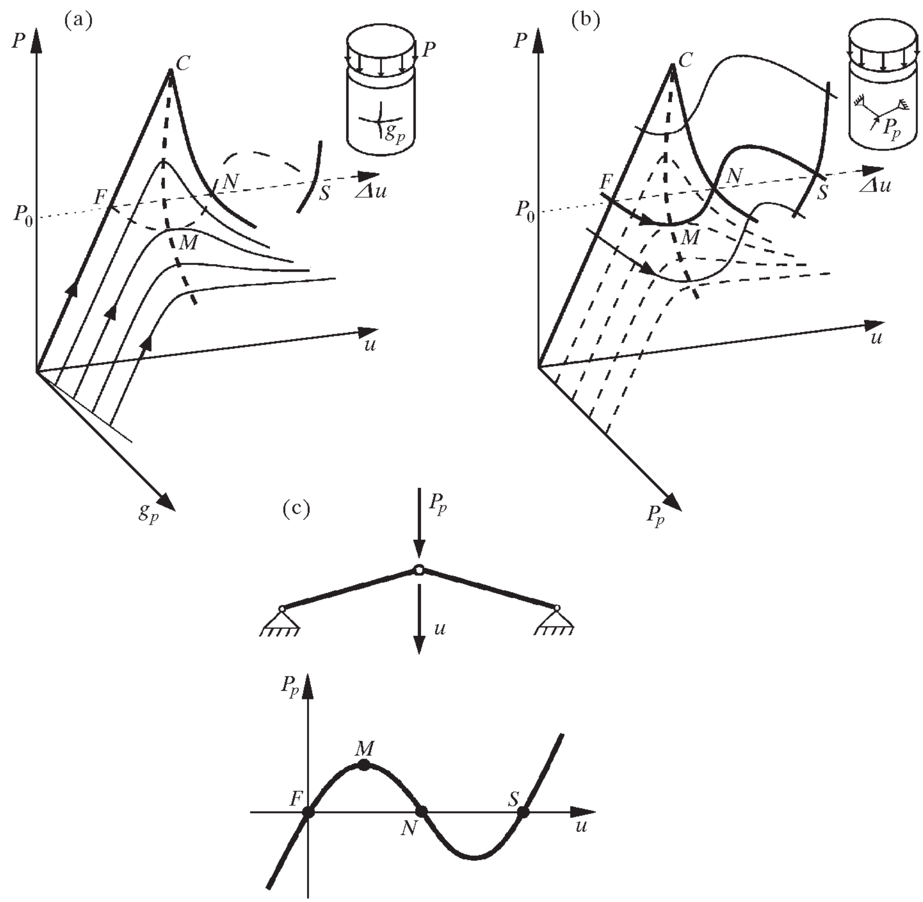

Fig. 1. Load-deformation behaviour of axially loaded cylindrical shells

the pre- to the post-buckling region, if the perturbation is large enough. This means that a limit state must exist between the pre- and post-buckling regions and it separates both regions. This limit state is the statically indifferent state of equilibrium with respect to the perturbations, M in Fig. 1. In the following it will be called a *critical state* of equilibrium and the strain energy that is stored by the structure during the deformation from the fundamental state of equilibrium F to the critical one M will be called the *critical strain energy* Π_{cr}. In the cases when the strain energy Π_p induced by perturbations is larger than the critical strain energy, the structure will buckle; otherwise it remains in the pre-buckling region

$$\Pi_p > \Pi_{cr} \quad \rightarrow \quad \text{buckling} \tag{3.1}$$

Thus, a perturbation theory may be established on the basis of the assumption of a potential, first for the elastic material behaviour. The total potential of the considered structures is split up to the strain energy and the external potential with respect to external actions

$$\Pi_{tot} = \Pi_{str} + \Pi_{ext} \tag{3.2}$$

The external potential is described by the design actions p_0 and the perturbations p_p

$$\Pi_{ext}(u, p_0, p_p) = -\int u(p_0 + p_p)\, dA \tag{3.3}$$

The principle of a stationary value of the potential leads to the equilibrium conditions, if its first variation with respect to the displacement field vanishes

$$\delta\Pi_{tot} = \delta u\Big(\frac{\partial\Pi_{str}}{\partial u} + \frac{\partial\Pi_{ext}}{\partial u}\Big) = 0 \tag{3.4}$$

Equation (3.4) may be used for computations of states of equilibrium with respect to p_0 or a perturbation load p_p, that belongs to the critical state $(p_0 + p_p, u_0 + u_p)$.

If the sensitivity of the ideal structure against perturbations is taken into account, the worst case of perturbations has to be investigated. The worst case is defined by the minimum of perturbation energy that may initiate buckling. This means that in addition to Eq. (3.4), the minimality condition for the potential with respect to perturbation loads must vanish

$$\delta\Pi_{tot} = u_p \delta p_p = 0 \tag{3.5}$$

as presented in Dinkler and Schäfer (1997). By means of Eq. (3.3) and (3.4), δp_p may be replaced by the displacement field u_p, that is conjugated to the perturbation load. From

$$p_p = \frac{\partial\Pi_{str}}{\partial u_p} \qquad \text{it follows that} \qquad \delta p_p = \delta u_p \frac{\partial}{\partial u_p}\Big(\frac{\partial\Pi_{str}}{\partial u_p}\Big) \tag{3.6}$$

Considering Eq. (3.6) in Eq.(3.5) yields the condition of the critical state of equilibrium for the worst perturbation

$$\delta u_p\Big(\frac{\partial^2\Pi_{str}}{\partial u_p^2}\Big)u_p = 0 \tag{3.7}$$

Physical meaning of this condition may be interpreted similarly to the snap-through behaviour: a state u_p has to be investigated, whereby the tangential stiffness at the state u_p in the direction of u_p vanishes.

The interpretation of Eq. (3.7) as a nonlinear eigenvalue problem is obvious, since the right-hand side vanishes and the coefficient of u_p depends on u_p itself. If the critical state is given by

$$u_{cr} = u_F + \lambda u_p \tag{3.8}$$

u_F holds the stable fundamental state of equilibrium and u_p – the normalized perturbation field, scaled by λ to the distance between u_F and the critical state. Considering Eq. (3.8) and Eq. (3.7), the nonlinear eigenvalue problem for the worst perturbation leads to

$$\delta u_p \Big[\frac{\partial^2 \varPi_{str}}{\partial u_p^2}(u_F) + \lambda \frac{\partial^2 \varPi_{str}^{NL}}{\partial u_p^2}(u_p)\Big] u_p = 0 \tag{3.9}$$

The first coefficient of Eq. (3.9) describes the tangential stiffness of the fundamental state of equilibrium, the second part the change of stiffness due to λu_p. If the critical deformation field λu_p is known, the critical strain energy $\varPi_{cr}$ depending on λu_p may be computed analogously to $\varDelta\varPi_{str}$.

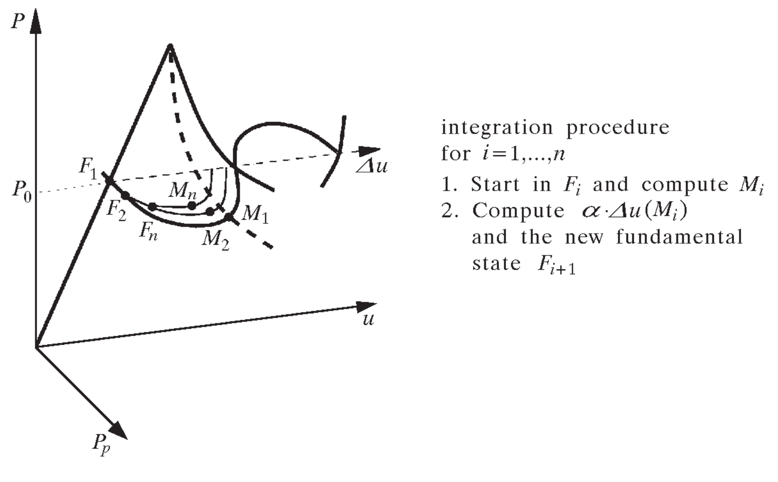

Fig. 2. Limit states for elasto-plastic material behaviour

In case of plastic material behaviour, the limit states depend on plastification. If the material starts yielding between the fundamental state of equilibrium and the critical state, the nonlinear eigenvalue problem, Eq. (3.9), has to be solved incrementally from the fundamental state to the critical state, with iterative correction of the plastic parts of the solution, see Fig. 2. The modified nonlinear eigenvalue problem may be written as

$$\delta u_p^{i+1}\Big[\frac{\partial^2 \varPi_{str}}{\partial u_p^2}(u_i,\varepsilon_i^{pl}) + \lambda_{i+1}\frac{\partial^2 \varPi_{str}^{NL}}{\partial u_p^2}(u_p^{i+1})\Big]u_p^{i+1} = 0 \tag{3.10}$$

with index i for the increment. Here

$$u_i = u_F + \sum \alpha\lambda_i u_p^i \qquad\qquad 0 < \alpha \leqslant 1.0 \tag{3.11}$$

is applied. α is a proper multiplier to scale the size of the increment. Eq. (3.10) has to be solved several times until the critical state is reached. Each intermediate state u_i, ε_i^{pl} has to satisfy all the governing equations and the yield condition, what is automatically achieved by the algorithm. In case of elasto-plastic material behaviour, the critical strain energy $\varPi_{cr}$ is the sum for each increment.

4. Application to cylindrical and conical shells

To obtain a proper buckling indicator for comparison of different shells and fundamental load conditions, the critical strain energy may be normalized by the bending stiffness, see Dinkler and Spohr (1998)

$$B = \frac{Et^3}{12(1-\nu^2)} \tag{4.1}$$

since buckling is directly connected to bending. The buckling indicator may be defined as

$$\pi_{cr} = \frac{\varPi_{cr}}{B} \tag{4.2}$$

Figure 3 presents numerical investigations for cylindrical and conical shells with various cone angles under axial compression in case of elastic material behaviour. Conical shells are represented at the slenderness r/t of the reference cylinder, where buckling occurs.

Normalized buckling loads for some values of the buckling indicator π_{cr} are shown in comparison with experiments and the German design rule DASt Ri 013. For the value of the buckling indicator π_{cr} of about $\pi_{cr} = 0.025$, numerical buckling loads for cylindrical and conical shells coincide extremely well with lower bounds of the experiments. However, the value of the buckling indicator, that fits the experiments, depends considerably on the discretisation

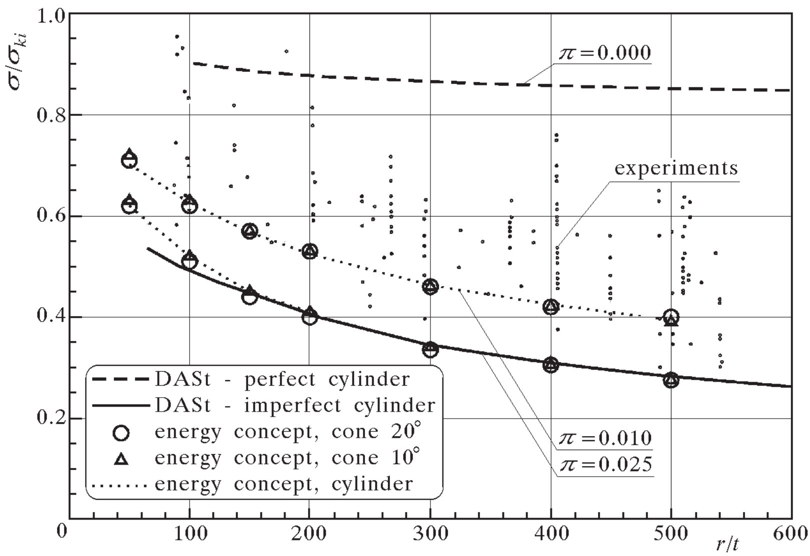

Fig. 3. Buckling loads of axially loaded shells in comparison to design rules DASt Ri 013

of the numerical computation, since local buckles need very fine meshes to be simulated. For short compact shells, the influence of boundary conditions on the buckling mode increases, what is considered directly by the buckling indicator π_{cr}. This may be the reason for the discrepancy with the empirical design values at this range of slenderness r/t.

Figure 4 presents the application of the concept to elasto-plastic buckling of cylindrical shells in comparison to the German design rule DIN 18800 and the European recommendations ECCS. The numerical results may be interpreted depending on the slenderness of shells. In case of small slenderness $\lambda_{Sx} < 0.4$ rotational elasto-plastic buckling leads to very high limit loads in comparison to the yield stress, since local buckling does not occur. Slender shells exhibit a purely elastic buckling behaviour as indicated in Fig. 3. For moderate slenderness $0.4 < \lambda_{Sx} < 1.25$, a mixed mode buckling occurs, where the procedure of Section 3.3 has to be applied. Nonetheless, the limit loads for shells with slenderness $\lambda_{Sx} < 0.5$ are below the minimum load capacity of the post-buckling region, where procedure 3.3 fails. In these cases the limit load is computed in the direction u_p of the lowest load level, where procedure 3.3 converges. A good coincidence of numerical results with the design rules is obvious.

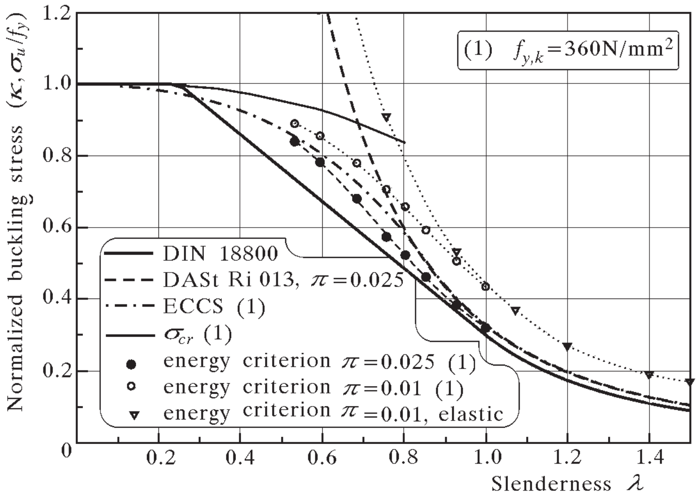

Fig. 4. Buckling loads of axially loaded shells in comparison to design rules

5. Application to combined shells

Combinations of single shells leading to combined shell structures yield a wide range of different shell types with different load-carrying and buckling behaviour. As the first example, unstiffened combinations of cylindrical and conical shells under axial compression are investigated. Fig. 5 shows the critical buckling shapes in case of an elastic material.

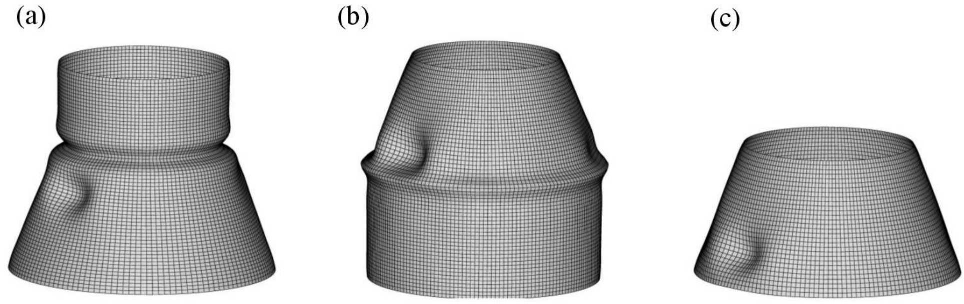

Fig. 5. Critical buckling shapes (a) concave cylinder-cone configuration, (b) convex configuration, (c) single conical shell, $\alpha = 20°$, $R'_{max} = 150$, $R'_{min} = 96$, $l = r$, $t_{cyl} = t_{cone}$

Without stiffeners at the cylinder-cone connections, the deformed configuration in the prebuckling region is dominated by large radial deformation at these connections. Concave connections show large inward-looking radial deformation. The resulting bending moments and circumferential forces are similar to single, simply supported shells. Convex connections, with outward-looking radial deformations, lead to contrary bending moments and circumferential forces. Nevertheless, the buckling shape for concave and convex connection is comparable to the single conical shell. It is a local buckle near the shell connection limited to the conical shell. Overall buckling does not occur.

Figure 6 shows the buckling loads of cylinder-cone configurations in comparison to the German design rule DASt Ri 013. The shells are represented at the slenderness r/t of the reference cylinder, where buckling occurs. The coincidence between the calculated buckling loads and the design rule is obvious, especially concave connections are comparable to single cylindrical or conical shells. The numerical buckling loads of convex connections show a slightly different behaviour, founded in the differences of deformation and stresses of the prebuckling region.

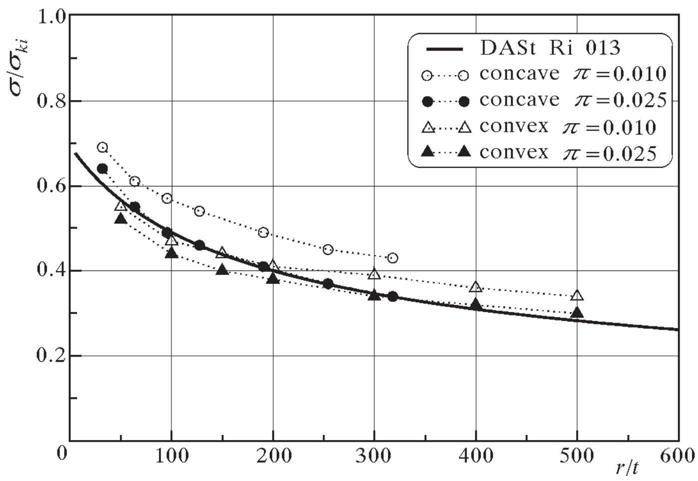

Fig. 6. Buckling loads of axially loaded cylinder-cone configurations

Elastic buckling of unstiffened cylinder-cone configurations is comparable to the buckling cases of single shells and the calculated limit loads are such high as the limit loads of stiffened structures. Expensive ring stiffeners are not necessary.

Figure 7a shows the load-deformation behaviour of an unstiffened cylinder-cone-cylinder configuration under axial compression for elastic and elasto-plastic material, experimental results from Swadlo (2001). In case of elasto-plastic material, the deformation behaviour is completely different from the

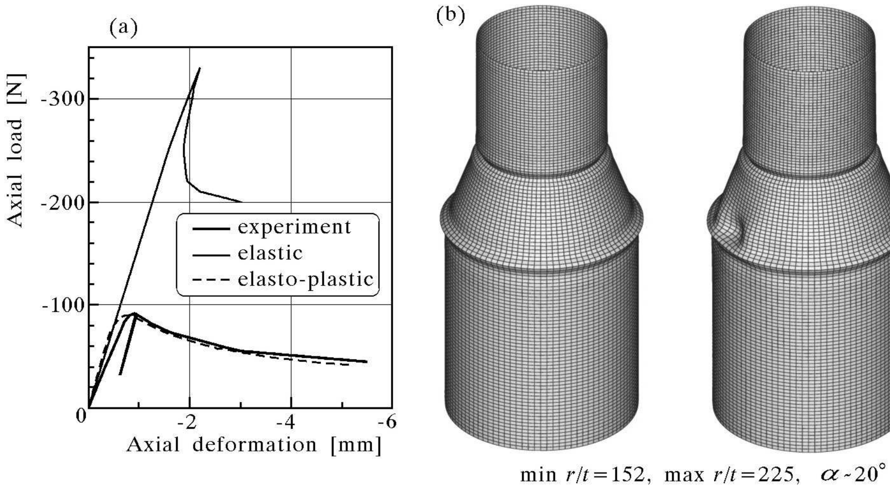

Fig. 7. Comparison of experiment, elastic and inelastic buckling behaviour, deformed configuration and critical buckling shape

case of elastic material. The ultimate load is much smaller than the bifurcation load and also the lower buckling load. There is no kind of snap-back in the load deformation path, rather a slow reduction of the ultimate load by increasing deformations.

The behaviour is caused by large radial deformations at the shell connections, which lead to high circumferential tension n_φ, see Fig. 8a. In connection with the axial compression forces n_α, material starts to yield at a very low load level compared to the stiffened structure, see Fig. 8c.

The failure of the entire structure is not a failure in terms of stability but rather a material failure at the shell connections. Coupled material and stability failure could only occur in case of very thin shells or material with high yield stress. To obtain the limit as high as those for single shells, ring stiffeners are necessary to reduce the circumferential tension stresses, what may help us to avoid the material failure at the shell connections.

6. Conclusions

The paper presents a procedure of evaluating imperfection sensitivity of shells and a buckling indicator for the design of shells. In contrast to other methods and failure criteria, it is not intended to get the lower bounds of the

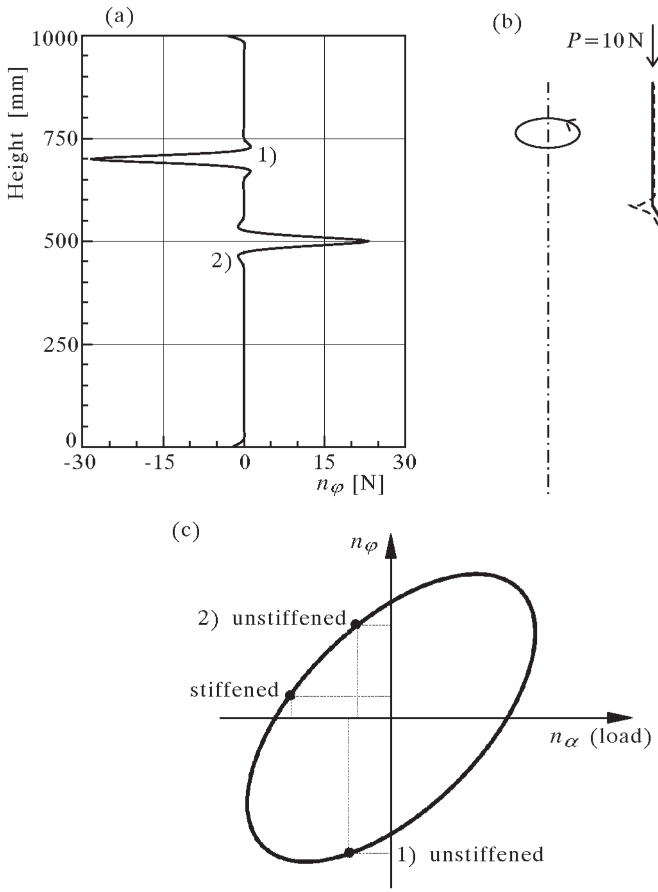

Fig. 8. Membrane forces and interaction

load deformation behaviour, but a comparison of the quantities of perturbation with experiments. So far, the authors know from literature the perturbation energy concept is the only concept, that is able to describe quality and quantity of the imperfection sensitivity of elasto-plastic buckling shells in very good agreement with experiments by means of a single scalar value π.

The concept is validated for buckling cases of cylindrical and conical shells. The coincidence between numerical results and the German design rule DASt Ri 013 is extremely good. In case of elasto-plastic behaviour, there is a good agreement between the numerical investigations and the European recommendations ECCS, what shows remarkable additional advantages of the German design rule DIN 18800.

In case of an elastic material, the buckling behaviour of unstiffened combined shells such as cylinder-cone configurations is comparable to the validated buckling cases of single shells. Limit loads of a unstiffened structures are such high as the limit loads of comparable stiffened structures. Expensive ring stiffeners are not necessary. Investigations concerning to inelastic buckling show a completely different failure modes as compared to single shells. Here, ring stiffeners at the shell connections are essential to increase the limit load of the entire structure and can not be neglected.

References

1. Arborcz J., Babcock C.D., 1969, The effect of general imperfections on the buckling of cylindrical shells, *Journ. Appl. Mech.*, 36
2. Budiansky B., 1974, Theory of Buckling and Post-Buckling behaviour of elastic structures, *Advances in Appl. Mech.*, 14
3. Budiansky B., Hutchinson J.W., 1966, A survey of some buckling problems, *AIAA Journal*, 4
4. Calladine C.R., 1995, Understanding imperfection-sensitivity in the buckling of thin-walled shells, *Thin-Walled Structures*, 23
5. Croll J.G.A., Batista R.C., 1981, Explicit lower bounds for the buckling of axially loaded cylinders, *Int. Journ. Mech. Sci.*, 23
6. Dinkler D., 1992, Phenomena in nonlinear dynamic buckling behaviour of elastic structures, *Proc. of the AIAA-Conference*, Dallas-Texas
7. Dinkler D., Schäfer U., 1997, Limit loads for cylindrical shells under combined actions, *Proc. Carrying capacity of steel shell structures*, Brno
8. Dinkler D., Spohr I., 1998, Elastic limit loads of cylindrical shells under combined axial and radial compression (in german), *Bauingenieur*, **73**, Springer Verlag
9. Duddeck H., Kröplin B., Dinkler D., Hillmann J., Wagenhuber W., 1990, Berechnung des nichtlinearen Tragverhaltens dünner Schalen im Vor- und Nachbeulbereich, *Nichtlineare Berechnungen im Konstruktiven Ingenieurbau*, Ed. E. Stein, Springer Verlag
10. Eggers H., Kröplin B., 1978, Yielding of plates with hardening and large deformations, *International Journal for numerical methods in engineering*, 12
11. Ilyushin A.A., 1947, The elasto-plastic stability of plates, *NACA Technical Memorandum*, 1188

12. Ilyushin A.A., 1956, *Plasticité*, Editions Eyrolles, Paris

13. von Kármán T., Tsien H.S., 1941, The buckling of thin cylindrical shells under axial compression, *Journal of Aeron. Sci.*, **8**

14. Koiter W.T., 1945, Over de stabiliteit van het elastisch evenwicht, Polytechnic Institut Delft, H.J. Paris Amsterdam, Engl. transl., 1967: On the stability of elastic equilibrium, NASA TT F-10

15. Koiter W.T., 1963, The effect of axisymmetric imperfections on the buckling of cylindrical shells under axial compression, *Proc. Kon. Ned. Akad. Wet.*, B66

16. Kröplin B., Dinkler D., Hillmann J., 1985, An energy perturbation applied to nonlinear structural analysis, *Computer Methods in Applied Mechanics and Engineering*, 52

17. Swadlo P., 2001, *Stabilität zusammengesetzter stählerner Kreiszylinder-Kegel-Schalen unter Axialdruck und Außendruck*, Essen

18. Yamaki N., 1984, *Elastic stability of cylindrical shells*, Horth-Holland

Sprężysto-plastyczne obciążenia graniczne w układach walcowo-stożkowych

Streszczenie

W pracy przedstawiono metodę wyznaczania obciążeń granicznych dla powłok wrażliwych na niedoskonałości, z uwzględnieniem odkształceń plastycznych. Opierając się na energii odkształcenia powłok rozważono przypadek najgorszego scenariusza krytycznych perturbacji przy ustalonych poziomach obciążeń. Wartości obciążeń granicznych dla powłok cylindrycznych i stożkowych porównano z przyjętymi w Europie metodami projektowania. Koncepcja została zastosowana do analizy bardziej ogólnych przypadków utraty stateczności konstrukcji powłokowych.

Manuscript received January 24, 2003; accepted for print March 5, 2003